



AFRL-RX-WP-JA-2014-0159

# ENGINEERING THE ACTIVITY AND LIFETIME OF HETEROGENEOUS CATALYSTS FOR CARBON NANOTUBE GROWTH VIA SUBSTRATE ION BEAM BOMBARDMENT (POSTPRINT)

B. Maruyama  
AFRL/RXAS

**AUGUST 2014**  
**Interim Report**

**Distribution A. Approved for public release; distribution unlimited.**

*See additional restrictions described on inside pages*

**STINFO COPY**

© 2014 American Chemical Society

**AIR FORCE RESEARCH LABORATORY  
MATERIALS AND MANUFACTURING DIRECTORATE  
WRIGHT-PATTERSON AIR FORCE BASE, OH 45433-7750  
AIR FORCE MATERIEL COMMAND  
UNITED STATES AIR FORCE**

## NOTICE AND SIGNATURE PAGE

Using Government drawings, specifications, or other data included in this document for any purpose other than Government procurement does not in any way obligate the U.S. Government. The fact that the Government formulated or supplied the drawings, specifications, or other data does not license the holder or any other person or corporation; or convey any rights or permission to manufacture, use, or sell any patented invention that may relate to them.

This report was cleared for public release by the USAF 88th Air Base Wing (88 ABW) Public Affairs Office (PAO) and is available to the general public, including foreign nationals.

Copies may be obtained from the Defense Technical Information Center (DTIC) (<http://www.dtic.mil>).

AFRL-RX-WP-JA-2014-0159 HAS BEEN REVIEWED AND IS APPROVED FOR PUBLICATION IN ACCORDANCE WITH ASSIGNED DISTRIBUTION STATEMENT.

---

//Signature//

BENJI MARUYAMA  
Soft Matter Materials Branch  
Functional Materials Division

---

//Signature//

KATIE E. THORP, Chief  
Soft Matter Materials Branch  
Functional Materials Division

---

//Signature//

TIMOTHY J. BUNNING, Chief  
Functional Materials Division  
Materials and Manufacturing Directorate

This report is published in the interest of scientific and technical information exchange, and its publication does not constitute the Government's approval or disapproval of its ideas or findings.

# REPORT DOCUMENTATION PAGE

Form Approved  
OMB No. 074-0188

Public reporting burden for this collection of information is estimated to average 1 hour per response, including the time for reviewing instructions, searching existing data sources, gathering and maintaining the data needed, and completing and reviewing this collection of information. Send comments regarding this burden estimate or any other aspect of this collection of information, including suggestions for reducing this burden to Defense, Washington Headquarters Services, Directorate for Information Operations and Reports, 1215 Jefferson Davis Highway, Suite 1204, Arlington, VA 22202-4302. Respondents should be aware that notwithstanding any other provision of law, no person shall be subject to any penalty for failing to comply with a collection of information if it does not display a currently valid OMB control number. PLEASE DO NOT RETURN YOUR FORM TO THE ABOVE ADDRESS.

1. REPORT DATE (DD-MM-YYYY) August 2014		2. REPORT TYPE Interim		3. DATES COVERED (From – To) 05 August 2010 – 18 July 2014	
4. TITLE AND SUBTITLE ENGINEERING THE ACTIVITY AND LIFETIME OF HETEROGENEOUS CATALYSTS FOR CARBON NANOTUBE GROWTH VIA SUBSTRATE ION BEAM BOMBARDMENT (POSTPRINT)				5a. CONTRACT NUMBER In-House	5b. GRANT NUMBER
				5c. PROGRAM ELEMENT NUMBER 62102F	5d. PROJECT NUMBER 4347
				5e. TASK NUMBER	5f. WORK UNIT NUMBER X0E8
6. AUTHOR(S) (see back)				8. PERFORMING ORGANIZATION REPORT NUMBER	
7. PERFORMING ORGANIZATION NAME(S) AND ADDRESS(ES) (see back)				10. SPONSOR/MONITOR'S ACRONYM(S) AFRL/RXAS	
9. SPONSORING / MONITORING AGENCY NAME(S) AND ADDRESS(ES) Air Force Research Laboratory Materials and Manufacturing Directorate Wright Patterson Air Force Base, OH 45433-7750 Air Force Materiel Command United States Air Force				11. SPONSOR/MONITOR'S REPORT NUMBER(S) AFRL-RX-WP-JA-2014-0159	
12. DISTRIBUTION / AVAILABILITY STATEMENT Distribution A. Approved for public release; distribution unlimited. This report contains color.					
13. SUPPLEMENTARY NOTES PA Case Number: 88ABW-2014-1004; Clearance Date: 11 March 2014. Journal article published in Nano Letters 2014, 14, 4997–5003. © 2014 American Chemical Society. The U.S. Government is joint author of the work and has the right to use, modify, reproduce, release, perform, display or disclose the work. The final publication is available at dx.doi.org/10.1021/nl501417h.					
14. ABSTRACT We demonstrate that argon ion bombardment of single crystal sapphire leads to the creation of substrates that support the growth of vertically aligned carbon nanotubes from iron catalysts with a density, height, and quality equivalent to those grown on conventional, disordered alumina supports. We quantify the evolution of the catalyst using a range of surface characterization techniques and demonstrate the ability to engineer and pattern the catalyst support through control of ion beam bombardment parameters.					
15. SUBJECT TERMS carbon nanotubes, heterogeneous catalyst, catalyst support, ion beam bombardment					
16. SECURITY CLASSIFICATION OF: Unclassified		17. LIMITATION OF ABSTRACT SAR	18. NUMBER OF PAGES 11	19a. NAME OF RESPONSIBLE PERSON (Monitor) Benji Maruyama	
a. REPORT Unclassified	b. ABSTRACT Unclassified	c. THIS PAGE Unclassified		19b. TELEPHONE NUMBER (include area code) (937) 255-0042	

## REPORT DOCUMENTATION PAGE Cont'd

### 6. AUTHOR(S)

B. Maruyama and S. L. Semiatin - Materials and Manufacturing Directorate, Air Force Research Laboratory, Functional Materials Division  
A. E. Islam, P. Nikolaev, and G. Sargent - Biological and Nanoscale Technologies, UES, Inc.  
P. B. Amama - Department of Chemical Engineering, Kansas State University  
S. Saber - School of Materials Science and Engineering, Purdue University  
D. Zakharov and E. A. Stach - Center for Functional Nanomaterials, Brookhaven National Laboratory  
D. Huffman - Department of Physics, Wright State University  
M. Erford - Southwestern Ohio Council for Higher Education

### 7. PERFORMING ORGANIZATION NAME(S) AND ADDRESS(ES)

AFRL/RXAS  
Air Force Research Laboratory  
Materials and Manufacturing Directorate  
Wright-Patterson Air Force Base, OH 45433-7750

Biological and Nanoscale Technologies  
UES, Inc.,  
Dayton, Ohio 45432

Department of Chemical Engineering  
Kansas State University  
Manhattan, Kansas 66506

School of Materials Science and Engineering  
Purdue University  
West Lafayette, Indiana 47907

Center for Functional Nanomaterials  
Brookhaven National Laboratory  
Upton, New York 11973

Department of Physics  
Wright State University  
Dayton, Ohio 45435

Southwestern Ohio Council for Higher Education  
Dayton, Ohio 45403

# Engineering the Activity and Lifetime of Heterogeneous Catalysts for Carbon Nanotube Growth via Substrate Ion Beam Bombardment

A. E. Islam,<sup>†,‡</sup> P. Nikolaev,<sup>†,‡</sup> P. B. Amama,<sup>§</sup> S. Saber,<sup>||</sup> D. Zakharov,<sup>⊥</sup> D. Huffman,<sup>†,‡,#</sup> M. Erford,<sup>▽</sup> G. Sargent,<sup>†,‡</sup> S. L. Semiatin,<sup>†</sup> E. A. Stach,<sup>⊥</sup> and B. Maruyama<sup>\*,†</sup>

<sup>†</sup>Materials and Manufacturing Directorate, Air Force Research Laboratory, Wright-Patterson Air Force Base, Dayton, Ohio 45433, United States

<sup>‡</sup>Biological and Nanoscale Technologies, UES, Inc., Dayton, Ohio 45432, United States

<sup>§</sup>Department of Chemical Engineering, Kansas State University, Manhattan, Kansas 66506, United States

<sup>||</sup>School of Materials Science and Engineering, Purdue University, West Lafayette, Indiana 47907, United States

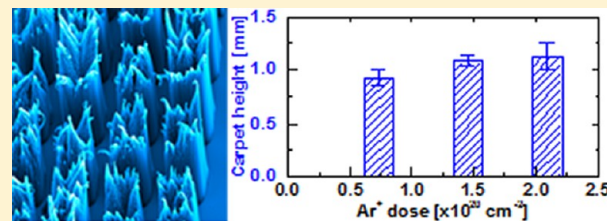
<sup>⊥</sup>Center for Functional Nanomaterials, Brookhaven National Laboratory, Upton, New York 11973, United States

<sup>#</sup>Department of Physics, Wright State University, Dayton, Ohio 45435, United States

<sup>▽</sup>Southwestern Ohio Council for Higher Education, Dayton, Ohio 45403, United States

## Supporting Information

**ABSTRACT:** We demonstrate that argon ion bombardment of single crystal sapphire leads to the creation of substrates that support the growth of vertically aligned carbon nanotubes from iron catalysts with a density, height, and quality equivalent to those grown on conventional, disordered alumina supports. We quantify the evolution of the catalyst using a range of surface characterization techniques and demonstrate the ability to engineer and pattern the catalyst support through control of ion beam bombardment parameters.



**KEYWORDS:** Carbon nanotubes, heterogeneous catalyst, catalyst support, ion beam bombardment

Carbon nanotubes (CNTs) have demonstrated unequalled structural,<sup>1–3</sup> transport,<sup>1,4–6</sup> and electronic/optoelectronic<sup>7</sup> properties. These properties have enabled the application of CNTs as ultralightweight composites in aerospace applications<sup>8–10</sup> and promise future applications such as electrical cables,<sup>1</sup> interconnects,<sup>11</sup> bio/chemical sensors,<sup>12,13</sup> energy storage devices,<sup>14–16</sup> field-emitting devices,<sup>1</sup> and high speed electronics.<sup>17–20</sup> The realization of these applications requires improvements in large-scale production of CNTs with sufficient control over yield,<sup>21–24</sup> density,<sup>11,25</sup> and chirality.<sup>19,20</sup> CNTs are grown via heterogeneous catalysis using a thin film of catalyst on a wide variety of catalyst supports. Films of transition metals like Fe, Co, and Ni generally form the most active catalyst nanoparticles for vertically aligned CNT (VA-CNT) growth.<sup>26,27</sup> The catalytic activity of these nanoparticles on solid supports is affected by water vapor<sup>21,22,28</sup> and carbon feedstock.<sup>23</sup> In addition, the catalytic activity is most efficient only on certain types of catalyst supports, specifically alumina or silica.<sup>29–36</sup> Even for materials like alumina or silica, only certain types of alumina,<sup>29–31,37,38</sup> quartz,<sup>39</sup> or sapphire<sup>40</sup> yield extended catalytic activity and hence longer VA-CNT growth.

Our previous study of alumina supports deposited by different methods clarified the role of the support in extending catalyst lifetime.<sup>29–31</sup> It was shown that while single-crystal, c-cut sapphire ( $\text{Al}_2\text{O}_3$ ) did not support VA-CNT growth,

substoichiometric alumina ( $\text{AlO}_x$ ) deposited by magnetron sputtering, electron beam evaporation, and atomic layer deposition (ALD) showed high levels of catalytic activity and CNT nucleation, resulting in  $\sim 10$ – $100 \mu\text{m}$  tall VA-CNT films. The key microstructural element for extending catalytic activity was established to be the porosity of the alumina support. Deposition techniques that led to higher porosity for the alumina support were shown to reduce coarsening of the deposited catalyst by inhibiting Ostwald ripening.<sup>28</sup>

Here we expand upon these insights and demonstrate that ion beam bombardment can be used to create catalyst supports with controllable degrees of catalytic activity and lifetime by generating a similar critical porosity and surface activity as that of conventional substrates.<sup>29–36</sup> Ion beam bombardment on crystalline substrates is generally known to introduce porosity at the top surface.<sup>41–43</sup> We have used this approach to convert an inactive catalyst support into a highly active support that results in a controlled level of vertically aligned growth using Fe as a catalyst. In this paper, we have chosen c-cut sapphire as the inactive catalyst support, as it shows insignificant VA-CNT growth<sup>29,40</sup> and hence provides a nice platform to engineer the

**Received:** April 16, 2014

**Revised:** July 18, 2014

**Published:** July 31, 2014

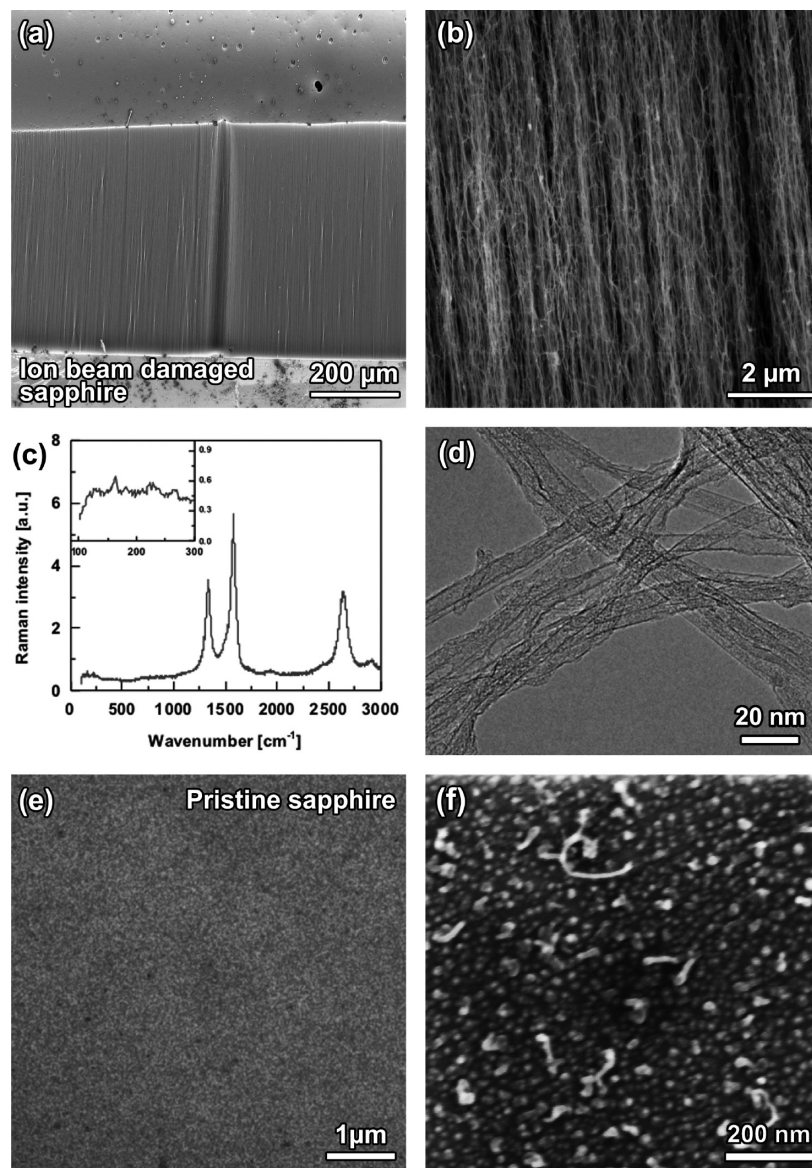


**Figure 1.** Ion beam bombarded sapphire catalyst supports grow tall vertically aligned carbon nanotube arrays. (a) Low- and (b) high-magnification SEM images showing  $\sim 0.8$  mm vertically aligned carbon nanotube (VA-CNT) growth using  $\sim 1$  nm Fe catalyst film on an ion beam damaged sapphire surface using  $\text{Ar}^+$  ion at a dose of  $\sim 2.1 \times 10^{20} \text{ cm}^{-2}$  and accelerated at 5 kV. (c) Raman spectra taken from the top of grown VA-CNT shows the presence of G' band, a G/D ratio of  $\sim 1.4$ , and radial breathing modes (inset) in the range of  $150$ – $300 \text{ cm}^{-1}$ . (d) Transmission electron microscopy image of grown CNT shows presence of single-wall, double-wall, and multiwall CNTs, along with amorphous carbon. In comparison to ion beam damaged sapphire, insignificant amount of CNTs are observed on pristine sapphire samples in the (e) low- and (f) high-magnification SEM images.

catalytic activity via ion beam bombardment. We utilize well-established characterization approaches to understand how the ion beam bombardment modifies the sapphire structure and improves the resultant catalytic activity. The method described herein expands the choice of catalyst supports, an important component for CNT growth, from a few types of alumina (determined by the deposition technique) to a continuum of engineered substrates.

To demonstrate the effectiveness of ion beam bombardment in growing VA-CNTs, we modified a c-cut sapphire substrate by bombarding it with 5 kV  $\text{Ar}^+$  ions at a dose of  $\sim 2.1 \times 10^{20} \text{ cm}^{-2}$  (see section S1 of Supporting Information for calculation of ion dose), then deposited  $\sim 1$  nm Fe film, and finally subjected the substrate to a CNT growth process, as elaborated in Methods. Figure 1a shows that the resulting VA-CNT films

are dense and well aligned with similar characteristics [e.g., overall carpet height ( $\sim 0.8$  mm) and Raman G/D ratio (1.4)] as we achieve using standard ALD alumina supports.<sup>29</sup> In comparison, a pristine sapphire sample (with no ion beam bombardment) subjected to the same growth conditions yielded only a few CNTs on the substrate and no vertically aligned growth (Figure 1e,f). The degree of VA-CNT growth in terms of carpet height (Figure 1a) and density (Figure 1b) is comparable to that obtained when using ALD or sputter-deposited  $\text{AlO}_x$  and lateral gas flow, although it is less than that obtained from showerhead growth.<sup>24</sup> Raman spectra taken from the top of the carpet (Figure 1c) suggests the presence of disordered CNTs with strong D and G' bands, with intensities comparable to that of the G band. The low G/D ratio ( $\sim 1.4$ ) from the Raman spectra is also an indicator of the abundance of

multiwalled CNTs in the samples,<sup>44,45</sup> a result that was confirmed using transmission electron microscopy (TEM) (Figure 1d). In addition, single-walled CNTs at the top of the carpet were observed via radial breathing mode (RBM) signals in the range of 150–300 cm<sup>-1</sup>.

Modification of the catalyst support via Ar<sup>+</sup> ion bombardment provides a novel way to pattern the catalyst activity by selectively masking certain parts of the sapphire from ion beam bombardment. Figure 2 shows VA-CNT growth in unmasked

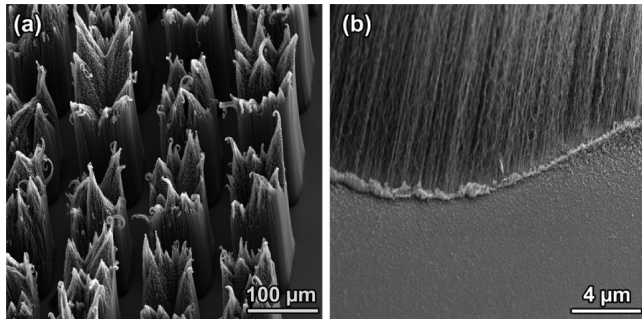


**Figure 2.** Demonstration of patterned VA-CNT growth via masked ion beam bombardment in selective regions of a sapphire substrate: (a) Low- and (b) high-magnification SEM images show VA-CNTs grown in patterned areas of a sapphire substrate, where ion beam damage was performed using a SiO<sub>x</sub>-coated Mo-TEM grid as shadow mask, while Fe catalyst was deposited all over the substrate.

areas of a sapphire substrate, where the catalyst support was modified via Ar<sup>+</sup> ion damage through a SiO<sub>x</sub>-coated Mo TEM grid that acted as a simple shadow mask. Despite the deposition of Fe catalyst (~1 nm Fe film) uniformly over the entire substrate, including the regions of pristine sapphire, only the

ion bombarded regions grew VA-CNTs. The approach, therefore, demonstrates the unique advantage of limiting growth only in Ar<sup>+</sup> ion damaged areas. In contrast, patterning the catalyst film deposition<sup>22,46</sup> to achieve selective area growth suffers from potential loss of fidelity in the pattern transfer via catalyst migration into regions outside the patterned area.

The catalyst supports that are currently used for VA-CNT growth<sup>29–36</sup> can be considered “static”, that is, the deposition method largely fixes their structure and activity. In contrast, ion beam bombardment enables continuous control over the structure of the catalyst support through independent control of the ion beam bombardment parameters. We explored the response of the catalyst support to changes in the ion beam accelerating voltage, as well as the ion beam dose. Figure 3a,b shows the measured height of VA-CNT carpets (like the one shown in Figure 1a) grown on sapphire surfaces damaged with varying ion beam parameters. Increased degrees of Ar<sup>+</sup> ion damage, caused by either increasing the accelerating voltage at a fixed damage dose (Figure 3a) or by increasing the damage dose at a fixed acceleration voltage (Figure 3b), results in higher carpet height. Observed variations in nanotube growth correlate nicely with the changes in catalyst morphology and also with the changes in both the structure and chemistry of the catalyst support.<sup>29–31</sup>

To monitor the changes in catalyst morphology, Ar<sup>+</sup> ion damaged sapphire substrates were coated with the same ~1 nm Fe catalyst film as used for nanotube growth and then annealed in H<sub>2</sub> ambient at 585 °C for 10 min. The resultant catalyst morphology replicates the condition at the onset of VA-CNT growth. Annealing of the catalyst film in an H<sub>2</sub> ambient induces dewetting and leads to the formation of iron nanoparticles on top of the engineered sapphire surfaces. Nanoparticles formed following a lower degree of Ar<sup>+</sup> ion damage (Figure 4a and

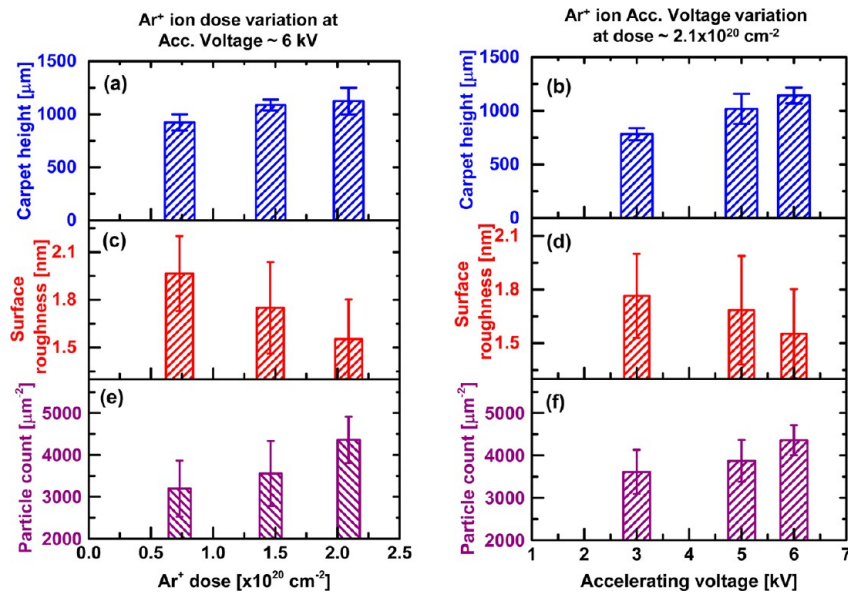


**Figure 3.** Control of VA-CNT growth and catalyst evolution via ion beam bombardment: Height of VA-CNT carpets grown on ion beam damaged sapphire substrates as a function of (a) Ar<sup>+</sup> ion dose at a fixed voltage and (b) accelerating voltage at a fixed dose. (c,d) Surface roughness and (e,f) nanoparticle density of the ripened catalyst on ion beam damaged sapphire substrates. These values were obtained via AFM (see Figure 4 and Supporting Information Figure S1 for example AFM images) after a sputter-deposited 1 nm Fe film on ion beam damaged sapphire was annealed in H<sub>2</sub> ambient at 585 °C for 10 min. For each ion beam bombardment conditions in (c–f), several (5–7) AFM topographies at different parts of the substrate were used to obtain the averages and standard deviations. Ion beam damage conditions for (c,e) and (d,f) are same as that for (a,b), respectively. Trends indicate that increasing damage, either via increase in dosage or increase in ion energy, results in similar improvement in VA-CNT growth and heterogeneous catalysis of Fe on sapphire.

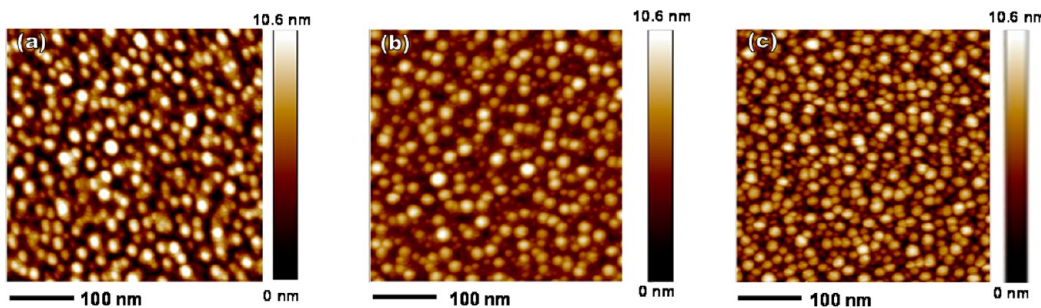


**Figure 4.** AFM topography of Fe nanoparticles on sapphire surfaces showing reduced Ostwald ripening rate with increased degree of damage: Sapphire surfaces were damaged using  $\text{Ar}^+$  ion at doses of (a)  $7 \times 10^{19} \text{ cm}^{-2}$ , (b)  $1.4 \times 10^{20} \text{ cm}^{-2}$ , and (c)  $2.1 \times 10^{20} \text{ cm}^{-2}$  at a fixed accelerating voltage of 6 kV. To form these nanoparticles on damaged sapphire surfaces, Fe film of  $\sim 1 \text{ nm}$  was coated on the surfaces, which was followed by a 10 min hydrogen anneal at  $585^\circ\text{C}$ . Catalyst particles show a reduction in size (with lower surface roughness) and increase in areal number density with increasing damage, as summarized in Figure 3c,e.

Supporting Information, Figure S1a) are larger and isolated, while those formed following higher degrees of  $\text{Ar}^+$  ion damage are smaller and are more closely spaced (Figure 4b,c and Supporting Information, Figure S1b,c). Atomic force microscopy (AFM) measurements of the ripened catalyst particles on the engineered surfaces exposed to higher degrees of  $\text{Ar}^+$  ion damage show lower surface roughness (Figure 3c,d) and higher particle number density (Figure 3e,f), both of which are known to enhance catalytic activity.<sup>29</sup> On the basis of our previous studies regarding catalyst morphology and carpet height,<sup>29–31,34,38</sup> the results in Figure 3 demonstrate control over the catalytic activity by controlling the Ostwald ripening rate.

In order to investigate the influence of the microstructure and surface properties on catalyst activity, we have used cross-sectional TEM (X-TEM) and X-ray photoelectron spectroscopy (XPS) to characterize the ion beam-damaged sapphire. The X-TEM image of an  $\text{Ar}^+$  ion engineered sapphire substrate (Figure 5) damaged with  $3.8 \times 10^{20} \text{ Ar}^+ \text{ ions/cm}^2$  at an

amorphous layer, followed by a nanocrystalline interfacial layer between the amorphous and crystalline regions (see Figure 5). This process has been studied extensively in the context of amorphous layer formation during ion implantation of both silicon and sapphire substrates.<sup>41–43</sup> Supporting Information Figure S3 presents X-ray reflection (XRR) data measured using  $\text{Cu K}\alpha$  radiation (wavelength,  $\lambda = 0.154 \text{ nm}$ ) on ion beam bombarded sapphire substrates prepared by varying  $\text{Ar}^+$  dose from  $1.4 \times 10^{19}$  to  $2.1 \times 10^{20} \text{ ions/cm}^2$  at an acceleration voltage of 5 kV. Analysis of XRR data reveals variation of damage layer thickness from  $\sim 9.4$  to  $\sim 12.8 \text{ nm}$  with the increase in ion beam damage dose. The lowest damage depth of  $\sim 9.4 \text{ nm}$  is comparable to the thickness of ALD alumina ( $\sim 10 \text{ nm}$ ) routinely used for VA-CNT growth.<sup>29–31,37,38</sup> This lowest ion beam damaged substrate resulted  $\sim 0.4 \text{ mm}$  tall VA-CNT carpet after completion of the catalyst annealing and the CNT growth phases. Experimental intricacy to produce a reliable beam current with shorter ion exposure inhibited us from determining the threshold dosage required for the initiation of VA-CNT growth.

Finally, XPS is used to characterize surface chemistry of the catalyst support following ion beam bombardment. Measurements of surface chemistry show good correlation with the catalyst activity. As has been recently shown,<sup>31</sup> deviations from  $\text{Al}_2\text{O}_3$  stoichiometry at the surface can be characterized by measuring the oxygen-to-aluminum (O/Al) ratio at the surface, while the surface active sites can be detected by monitoring the increase in surface-active oxygen species relative to stable oxygen. Figure 6a,b presents the ratios of the O 1s ( $\text{O}_2^-$  component) peak area to the Al 2p peak area and the full width at half-maximum (FWHM) for the O 1s peak, respectively, for sapphire surfaces that were damaged at different degrees of  $\text{Ar}^+$  ion bombardment by varying the acceleration voltage. Figure 6c–e shows how the O 1s spectra obtained for different sapphire surfaces are decomposed into contributions from  $\text{OH}^-$  (with a peak at  $\sim 532.1 \pm 0.2 \text{ eV}$ ) and  $\text{O}_2^-$  (with a peak at  $\sim 530.9 \pm 0.2 \text{ eV}$ ), which is important for the correct extraction of the O/Al ratio and the FWHM.<sup>47</sup> The values obtained for the O/Al ratio and FWHM of our engineered catalyst supports are consistent with similar values (dotted lines in Figure 6a,b) recently measured for ALD- $\text{AlO}_x$ ,<sup>31,47</sup> which is routinely used as catalyst support for VA-CNT growth. An increase in both the O/Al atomic ratio and the O 1s peak width with the increase in ion beam damage suggests a hydroxyl enrichment on the engineered sapphire surface, which can be correlated with the higher degree of catalytic activity<sup>31</sup> and longer lifetime of the Fe

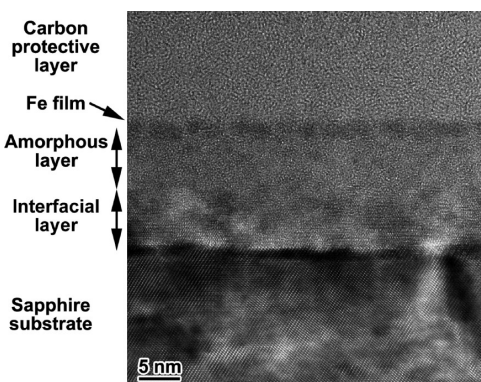


**Figure 5.** Cross-section TEM image of an ion beam damaged sapphire substrate: The substrate was bombarded with  $3.8 \times 10^{20} \text{ Ar}^+ \text{ ions/cm}^2$  at an acceleration voltage of 5 kV and then coated with a  $\sim 1 \text{ nm}$  Fe film. TEM image shows the creation of amorphous and nanocrystalline interfacial layers on top of crystalline sapphire with a total damage depth of  $\sim 13 \text{ nm}$ .

acceleration voltage of 5 kV shows the presence of  $\sim 13 \text{ nm}$  thick damaged layer near the surface of the substrate that acts as the porous catalyst support. (Supporting Information Figure S2 illustrates how energy filtered maps of iron, carbon, and oxygen were used to identify different regions of Figure 5.)  $\text{Ar}^+$  ion damage presumably results in epitaxial regrowth of an

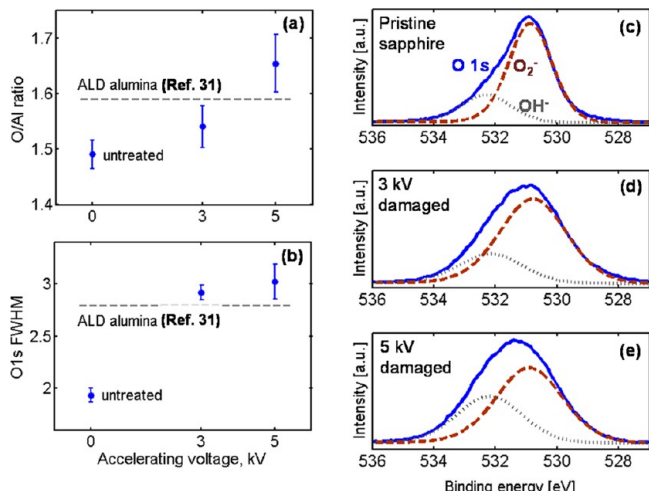


**Figure 6.** Comparison of ALD alumina and ion beam damaged sapphire surfaces via XPS shows a controlled increase in surface activity with increase ion beam damage: (a) the ratios of the O 1s ( $O_2^-$  component) peak area to the Al 2p peak area (O/Al ratio) and (b) FWHM for the O 1s peak for engineered sapphire surfaces with increasing degrees of  $Ar^+$  ion bombardment. To calculate the O/Al ratio, each O 1s spectra is decomposed into contributions from  $OH^-$  and  $O_2^-$ . Such decomposition is shown for the O 1s spectra obtained at the surface of (c) pristine sapphire and  $Ar^+$  ion damaged sapphire at (d) 3 and (e) 5 kV accelerating voltage. These XPS results demonstrate the ability of ion beam damage to engineer the catalyst support surface over a wide range of conditions.

catalyst nanoparticles formed on the damaged substrate surface. We can thus conclude that the  $Ar^+$  ion bombardment makes the sapphire surface nonstoichiometric and enriched in hydroxyl groups and introduces the disorder that has been shown to enhance catalytic activity and lifetime.

In conclusion, a new approach<sup>48</sup> has been developed to transform a relatively inert sapphire substrate into a highly active catalyst support that enables supergrowth of carbon nanotubes. The resultant supports grow nanotubes with a density, height, and quality equivalent to those obtained from conventional, vapor-deposited alumina-based catalyst supports. The correlation between the observed formation of surfaces that are disordered, nonstoichiometric, and enriched in hydroxyl groups is consistent with and further validates our understanding of the roles Ostwald ripening, coarsening, and surface chemistry as the defining mechanisms for nanotube growth.<sup>28–31</sup> The contrast between the vertically aligned CNT growth on areas bombarded with  $Ar^+$  ions and the lack of growth on the pristine substrate highlights the sharp difference in catalyst dynamics between an atomically perfect surface and an intentionally disrupted one. The ion beam bombardment method of modifying catalyst supports enables one to engineer the degree of catalyst activation through control of the ion beam energy, dose, and spatial patterning. These results can be complimented by the rich literature concerning ion beam processing of surface to further understand, improve, and control nanotube growth for electronic and thermal applications. Finally, these results indicate that ion bombardment can be considered as yet another method in catalysis science to engineer supports to enhance both catalytic activity and lifetime with general implications for heterogeneous catalysis.<sup>49,50</sup>

**Methods. Experiment.** For VA-CNT growth on crystalline c-cut sapphire substrates, the substrates were bombarded with

argon ions ( $Ar^+$ ) accelerated at 3–6 kV and at variable ion fluxes ( $0.7$ – $2.1 \times 10^{20} \text{ cm}^{-2}$ ). A thin film ( $\sim 1 \text{ nm}$ ) of Fe was deposited via ion beam sputtering on the  $Ar^+$  ion-damaged samples as the source of catalyst for VA-CNT growth. The Fe-deposited,  $Ar^+$  ion-damaged samples were annealed in hydrogen ambient (200 sccm flow) at  $585^\circ\text{C}$  for 10 min to dewet the catalyst layer into discrete nanoparticles. The samples were then rapidly cooled down to room temperature in a hydrogen ambient. Some samples were removed from the reactor at this point to characterize the degree of catalyst evolution using atomic force microscopy (AFM). Other samples were immediately subjected to growth conditions at  $760^\circ\text{C}$  for 30 min, at a water concentration of 50–80 ppm, and gas flow rates of 470, 100, and 25 sccm for argon, hydrogen, and ethylene, respectively. Grown nanotubes were analyzed using scanning electron microscopy (SEM), Raman spectroscopy, and transmission electron microscopy (TEM) for qualitative and quantitative analyses. In addition, surface properties of the ion beam-bombarded catalyst support were characterized using AFM and X-ray photoelectron spectroscopy (XPS), and the degree of  $Ar^+$  ion damage was characterized using cross-sectional TEM. XPS analysis was performed using a Surface Science Instruments (SSI) M-probe equipped with an Al  $K\alpha$  X-ray source (operated at  $\sim 4 \times 10^{-7} \text{ Pa}$  base pressure) and collected data were analyzed using CASA XPS software using Shirley background subtraction. AFM was carried out in a Veeco Nanoscope Multimode instrument using MikroMasch HQ:NSC15/Al-BS (having tip radius  $\sim 8 \text{ nm}$ , resonant frequency 265–410 kHz, and force constant 20–80 N/m). TEM studies were performed in a FEI Titan Environmental TEM at an accelerating voltage of 300 kV.

## ■ ASSOCIATED CONTENT

### § Supporting Information

The calculation procedure of ion beam damage dose, example AFM images analyzed to calculate surface roughness and nanoparticle density in Figure 3d,f, energy-filtered TEM images showing the amount of chemical species at different locations of Figure 5, and the analysis of ion beam damaged layers on the surface of c-cut sapphire using X-ray reflectivity measurements for different ion damage dose are presented. This material is available free of charge via the Internet at <http://pubs.acs.org>.

## ■ AUTHOR INFORMATION

### Corresponding Author

\*E-mail: benji.maruyama@us.af.mil.

### Author Contributions

A.E.I. and P.N. contributed equally in this manuscript. The manuscript was written through contributions of all authors. All authors have given approval to the final version of the manuscript.

### Notes

The authors declare no competing financial interest.

## ■ ACKNOWLEDGMENTS

This work was supported by the Air Force Office of Scientific Research, under Contract No. FA 8650-09-D-5037. Research carried out in part at the Center for Functional Nanomaterials, Brookhaven National Laboratory, which is supported by the U.S. Department of Energy, Office of Basic Energy Sciences, under Contract No. DE-AC02-98CH10886. S.S. acknowledges

partial support from the Purdue Electron Microscopy Consortium.

## ■ REFERENCES

- (1) Behabtu, N.; Young, C. C.; Tsentalovich, D. E.; Kleinerman, O.; Wang, X.; Ma, A. W. K.; Bengio, E. A.; ter Waarbeek, R. F.; de Jong, J.; Hoogerwerf, R. E.; et al. Strong, Light, Multifunctional Fibers of Carbon Nanotubes with Ultrahigh Conductivity. *Science* **2013**, *339*, 182–186.
- (2) Qu, L.; Dai, L.; Stone, M.; Xia, Z.; Wang, Z. L. Carbon nanotube arrays with strong shear binding-on and easy normal lifting-off. *Science* **2008**, *322*, 238–242.
- (3) Wong, E. W.; Sheehan, P. E.; Lieber, C. M. Nanobeam mechanics: Elasticity, strength, and toughness of nanorods and nanotubes. *Science* **1997**, *277*, 1971–1975.
- (4) Pop, E.; Mann, D.; Wang, Q.; Goodson, K. E.; Dai, H. J. Thermal Conductance of an Individual Single-Wall Carbon Nanotube above Room Temperature. *Nano Lett.* **2006**, *6*, 96–100.
- (5) Zhou, X. J.; Park, J. Y.; Huang, S. M.; Liu, J.; McEuen, P. L. Band structure, phonon scattering, and the performance limit of single-walled carbon nanotube transistors. *Phys. Rev. Lett.* **2005**, *95*.
- (6) Yao, Z.; Kane, C. L.; Dekker, C. High-field electrical transport in single-wall carbon nanotubes. *Phys. Rev. Lett.* **2000**, *84*, 2941–2944.
- (7) Avouris, P.; Freitag, M.; Perebeinos, V. Carbon-nanotube photonics and optoelectronics. *Nat. Photonics* **2008**, *2*, 341–350.
- (8) Breuer, O.; Sundararaj, U. Big returns from small fibers: A review of polymer/carbon nanotube composites. *Polym. Compos.* **2004**, *25*, 630–645.
- (9) De Rosa, I. M.; Sarasini, F.; Sarto, M. S.; Tamburrano, A. EMC impact of advanced carbon fiber/carbon nanotube reinforced composites for next-generation aerospace applications. *IEEE Trans. Electromagn. Compat.* **2008**, *50*, 556–563.
- (10) Sandler, J. K. W.; Kirk, J. E.; Kinloch, I. A.; Shaffer, M. S. P.; Windle, A. H. Ultra-low electrical percolation threshold in carbon-nanotube-epoxy composites. *Polymer* **2003**, *44*, 5893–5899.
- (11) Esconjauregui, S.; Fouquet, M.; Bayer, B. C.; Ducati, C.; Smajda, R.; Hofmann, S.; Robertson, J. Growth of Ultrahigh Density Vertically Aligned Carbon Nanotube Forests for Interconnects. *ACS Nano* **2010**, *4*, 7431–7436.
- (12) Pengfei, Q. F.; Vermesh, O.; Grecu, M.; Javey, A.; Wang, O.; Dai, H. J.; Peng, S.; Cho, K. J. Toward Large Arrays of Multiplex Functionalized Carbon Nanotube Sensors for Highly Sensitive and Selective Molecular Detection. *Nano Lett.* **2003**, *3*, 347–351.
- (13) Collins, P. G.; Bradley, K.; Ishigami, M.; Zettl, A. Extreme oxygen sensitivity of electronic properties of carbon nanotubes. *Science* **2000**, *287*, 1801–1804.
- (14) Cao, Z.; Wei, B. A perspective: carbon nanotube macro-films for energy storage. *Energy Environ. Sci.* **2013**, *6*, 3183–3201.
- (15) Dillon, A. C. Carbon Nanotubes for Photoconversion and Electrical Energy Storage. *Chem. Rev.* **2010**, *110*, 6856–6872.
- (16) Zhang, Q.; Huang, J.-Q.; Qian, W.-Z.; Zhang, Y.-Y.; Wei, F. The Road for Nanomaterials Industry: A Review of Carbon Nanotube Production, Post-Treatment, and Bulk Applications for Composites and Energy Storage. *Small* **2013**, *9*, 1237–1265.
- (17) Avouris, P. Nanotube electronics - Electronics with carbon nanotubes. *Phys. World* **2007**, *20*, 40–45.
- (18) Cao, Q.; Han, S.-j. Single-walled carbon nanotubes for high-performance electronics. *Nanoscale* **2013**, *5*, 8852–8863.
- (19) Cao, Q.; Han, S.-j.; Tulevski, G. S.; Zhu, Y.; Lu, D. D.; Haensch, W. Arrays of single-walled carbon nanotubes with full surface coverage for high-performance electronics. *Nat. Nanotechnol.* **2013**, *8*, 180–186.
- (20) Jin, S. H.; Dunham, S. N.; Song, J.; Xie, X.; Kim, J.-H.; Lu, C.; Islam, A.; Du, F.; Kim, J.; Felts, J.; et al. Using nanoscale thermocapillary flows to create arrays of purely semiconducting single-walled carbon nanotubes. *Nat. Nanotechnol.* **2013**, *8*, 347–355.
- (21) Hasegawa, K.; Noda, S. Millimeter-Tall Single-Walled Carbon Nanotubes Rapidly Grown with and without Water. *ACS Nano* **2011**, *5*, 975–984.
- (22) Hata, K.; Futaba, D. N.; Mizuno, K.; Namai, T.; Yumura, M.; Iijima, S. Water-assisted highly efficient synthesis of impurity-free single-walled carbon nanotubes. *Science* **2004**, *306*, 1362–1364.
- (23) Kimura, H.; Goto, J.; Yasuda, S.; Sakurai, S.; Yumura, M.; Futaba, D. N.; Hata, K. Unexpectedly High Yield Carbon Nanotube Synthesis from Low-Activity Carbon Feedstocks at High Concentrations. *ACS Nano* **2013**, *7*, 3150–3157.
- (24) Yasuda, S.; Futaba, D. N.; Yamada, T.; Satou, J.; Shibuya, A.; Takai, H.; Arakawa, K.; Yumura, M.; Hata, K. Improved and Large Area Single-Walled Carbon Nanotube Forest Growth by Controlling the Gas Flow Direction. *ACS Nano* **2009**, *3*, 4164–4170.
- (25) Naeemi, A.; Meindl, J. D. Design and performance modeling for single-walled carbon nanotubes as local, semiglobal, and global interconnects in gigascale integrated systems. *IEEE Trans. Electron Devices* **2007**, *54*, 26–37.
- (26) Hafner, J. H.; Bronikowski, M. J.; Azamian, B. R.; Nikolaev, P.; Rinzler, A. G.; Colbert, D. T.; Smith, K. A.; Smalley, R. E. Catalytic growth of single-wall carbon nanotubes from metal particles. *Chem. Phys. Lett.* **1998**, *296*, 195–202.
- (27) Yuan, D.; Ding, L.; Chu, H.; Feng, Y.; McNicholas, T. P.; Liu, J. Horizontally Aligned Single-Walled Carbon Nanotube on Quartz from a Large Variety of Metal Catalysts. *Nano Lett.* **2008**, *8*, 2576–2579.
- (28) Amama, P. B.; Pint, C. L.; McJilton, L.; Kim, S. M.; Stach, E. A.; Murray, P. T.; Hauge, R. H.; Maruyama, B. Role of Water in Super Growth of Single-Walled Carbon Nanotube Carpets. *Nano Lett.* **2009**, *9*, 44–49.
- (29) Amama, P. B.; Pint, C. L.; Kim, S. M.; McJilton, L.; Eyink, K. G.; Stach, E. A.; Hauge, R. H.; Maruyama, B. Influence of Alumina Type on the Evolution and Activity of Alumina-Supported Fe Catalysts in Single-Walled Carbon Nanotube Carpet Growth. *ACS Nano* **2010**, *4*, 895–904.
- (30) Amama, P. B.; Pint, C. L.; Mirri, F.; Pasquali, M.; Hauge, R. H.; Maruyama, B. Catalyst-support interactions and their influence in water-assisted carbon nanotube carpet growth. *Carbon* **2012**, *50*, 2396–2406.
- (31) Amama, P. B.; Putnam, S. A.; Barron, A. R.; Maruyama, B. Wetting behavior and activity of catalyst supports in carbon nanotube carpet growth. *Nanoscale* **2013**, *5*, 2642–2646.
- (32) de los Arcos, T.; Garnier, M. G.; Oelhafen, P.; Mathys, D.; Seo, J. W.; Domingo, C.; Garcí-Ramos, J. V.; Sanchez-Cortes, S. Strong influence of buffer layer type on carbon nanotube characteristics. *Carbon* **2004**, *42*, 187–190.
- (33) Han, S. J.; Yu, T. K.; Park, J.; Koo, B.; Joo, J.; Hyeon, T.; Hong, S.; Im, J. Diameter-Controlled Synthesis of Discrete and Uniform-Sized Single-Walled Carbon Nanotubes Using Monodisperse Iron Oxide Nanoparticles Embedded in Zirconia Nanoparticle Arrays as Catalysts. *J. Phys. Chem. B* **2004**, *108*, 8091–8095.
- (34) Kim, S. M.; Pint, C. L.; Amama, P. B.; Hauge, R. H.; Maruyama, B.; Stach, E. A. Catalyst and catalyst support morphology evolution in single-walled carbon nanotube supergrowth: Growth deceleration and termination. *J. Mater. Res.* **2010**, *25*, 1875–1885.
- (35) Mattevi, C.; Wirth, C. T.; Hofmann, S.; Blume, R.; Cantoro, M.; Ducati, C.; Cepek, C.; Knop-Gericke, A.; Milne, S.; Castellarin-Cudia, C.; et al. In-Situ X-ray Photoelectron Spectroscopy Study of Catalyst-Support Interactions and Growth of Carbon Nanotube Forests. *J. Phys. Chem. C* **2008**, *112*, 12207–12213.
- (36) Wang, B.; Yang, Y.; Li, L.-J.; Chen, Y. Effect of different catalyst supports on the (n,m) selective growth of single-walled carbon nanotube from Co-Mo catalyst. *J. Mater. Sci.* **2009**, *44*, 3285–3295.
- (37) Kim, S. M.; Pint, C. L.; Amama, P. B.; Zakharov, D. N.; Hauge, R. H.; Maruyama, B.; Stach, E. A. Understanding Growth Termination of Single-Walled Carbon Nanotube Carpets by Documenting the Evolution of Catalyst Morphology with the Transmission Electron Microscope. *Microsc. Microanal.* **2009**, *15*, 1176–1177.
- (38) Kim, S. M.; Pint, C. L.; Amama, P. B.; Zakharov, D. N.; Hauge, R. H.; Maruyama, B.; Stach, E. A. Evolution in Catalyst Morphology Leads to Carbon Nanotube Growth Termination. *J. Phys. Chem. Lett.* **2010**, *1*, 918–922.

(39) Murakami, Y.; Chiashi, S.; Miyauchi, Y.; Hu, M. H.; Ogura, M.; Okubo, T.; Maruyama, S. Growth of vertically aligned single-walled carbon nanotube films on quartz substrates and their optical anisotropy. *Chem. Phys. Lett.* **2004**, *385*, 298–303.

(40) Ohno, H.; Takagi, D.; Yamada, K.; Chiashi, S.; Tokura, A.; Homma, Y. Growth of vertically aligned single-walled carbon nanotubes on alumina and sapphire substrates. *Jpn. J. Appl. Phys.* **2008**, *47*, 1956–1960.

(41) Linnros, J.; Svensson, B.; Holmen, G. Ion-beam-induced Epitaxial Regrowth of Amorphous Layers in Silicon on Sapphire. *Phys. Rev. B* **1984**, *30*, 3629–3638.

(42) Canut, B.; Benyagoub, A.; Marest, G.; Meftah, A.; Moncoffre, N.; Ramos, S. M. M.; Studer, F.; Thevenard, P.; Toulemonde, M. Swift-Uranium-ion-induced Damage in Sapphire. *Phys. Rev. B* **1995**, *51*, 12194–12201.

(43) Golecki, I.; Chapman, G. E.; Lau, S. S.; Tsaur, B. Y.; Mayer, J. W. Ion-beam Induced Epitaxy of Silicon. *Phys. Lett. A* **1979**, *71*, 267–269.

(44) Eswaraiah, V.; Sankaranarayanan, V.; Ramaprabhu, S. Inorganic nanotubes reinforced polyvinylidene fluoride composites as low-cost electromagnetic interference shielding materials. *Nanoscale Res. Lett.* **2011**, *6*, 137.

(45) Chakrabarti, S.; Kume, H.; Pan, L.; Nagasaka, T.; Nakayama, Y. Number of Walls Controlled Synthesis of Millimeter-Long Vertically Aligned Brushlike Carbon Nanotubes. *J. Phys. Chem. C* **2007**, *111*, 1929–1934.

(46) Yun, Y.; Shanov, V.; Tu, Y.; Subramaniam, S.; Schulz, M. J. Growth Mechanism of Long Aligned Multiwall Carbon Nanotube Arrays by Water-Assisted Chemical Vapor Deposition. *J. Phys. Chem. B* **2006**, *110*, 23920–23925.

(47) van den Brand, J.; Sloof, W. G.; Terryn, H.; de Wit, J. H. W. Correlation between hydroxyl fraction and O/Al atomic ratio as determined from XPS spectra of aluminium oxide layers. *Surf. Interface Anal.* **2004**, *36*, 81–88.

(48) Maruyama, B.; Sargent, G.; Islam, A. E. *Methods of Enhancing Carbon Nanotube Growth on Substrates*. Patent Pending.

(49) Lu, J.; Fu, B.; Kung, M. C.; Xiao, G.; Elam, J. W.; Kung, H. H.; Stair, P. C. Coking- and Sintering-Resistant Palladium Catalysts Achieved Through Atomic Layer Deposition. *Science* **2012**, *335*, 1205–1208.

(50) Park, J. B.; Graciani, J.; Evans, J.; Stacchiola, D.; Ma, S.; Liu, P.; Nambu, A.; Fernandez Sanz, J.; Hrbek, J.; Rodriguez, J. A. High catalytic activity of Au/CeO<sub>x</sub>/TiO<sub>2</sub>(110) controlled by the nature of the mixed-metal oxide at the nanometer level. *Proc. Natl. Acad. Sci. U.S.A.* **2009**, *106*, 4975–4980.

### ■ NOTE ADDED IN PROOF

A recent publication has also demonstrated the utility of oxygen plasma bombardment in aiding VA-CNT growth. See J. Yang, et al., *J. Phys. Chem. C*, Article ASAP, DOI: 10.1021/jp5022196.